Molecular Pharmacology Fast Forward. Published on April 21, 2014 as doi:10.1124/mol.114.091926
This article has not been copyedited and formatted. The final version may differ from this version.

MOL #91926

AN N-TERMINAL THREONINE MUTATION PRODUCES AN EFFLUX FAVORABLE, SODIUM-PRIMED CONFORMATION OF THE HUMAN DOPAMINE TRANSPORTER

Rheaclare Fraser, Yongyue Chen, Bipasha Guptaroy, Kathryn D. Luderman, Stephanie L. Stokes, Asim Beg, Louis J. DeFelice, and Margaret E. Gnegy

Department of Physiology and Biophysics (L.J.D.), Department of Psychiatry (Y.C.), Virginia Commonwealth University, Richmond VA 23220

Department of Pharmacology University of Michigan, Ann Arbor, MI 48019 (R.F., B.G., K.D.L., S.L.S., A.B., and M.E.G.)

Molecular Pharmacology Fast Forward. Published on April 21, 2014 as DOI: 10.1124/mol.114.091926
This article has not been copyedited and formatted. The final version may differ from this version.

MOL #91926

Running title: A Sodium-primed and Efflux-favorable Conformation of DAT

Corresponding Author:

Margaret E. Gnegy

Department of Pharmacology, 2220E MSRBIII

University of Michigan Medical School

1150 West Medical Center Drive

Ann Arbor, MI 48109-0632

Telephone: 734-763-5358

Fax: 734-763-4450

Email: pgnegy@umich.edu

Text pages: 34

Figures: 7

Tables: 0

References: 42

Number of words:

Abstract: 248 words

Introduction: 684 words

Discussion: 1428 words

Abbreviations: AMPH, amphetamine; ASP^+, 4-(4-(dimethylamino)styryl)-N-methylpyridinium); DA, dopamine; HEK, human embryonic kidney cells; hDAT, human dopamine transporter; KRH, Krebs-Ringer Hepes buffer; Na^+_e, extracellular sodium; NMDG-Cl, *N*-methyl-D-glucamine chloride; TM, transmembrane domain

Molecular Pharmacology Fast Forward. Published on April 21, 2014 as DOI: 10.1124/mol.114.091926
This article has not been copyedited and formatted. The final version may differ from this version.

ABSTRACT

The dopamine transporter (DAT) reversibly transports dopamine (DA) through a series of conformational transitions. Alanine (T62A) or aspartate (T62D) mutagenesis of Thr 62 revealed T62D-hDAT partitions in a predominately efflux-preferring conformation. Compared to wild type (WT), T62D-hDAT exhibits reduced [^{3}H]DA uptake and enhanced baseline DA efflux, while T62A-hDAT and WT-hDAT function in an influx-preferring conformation. We now interrogate the basis of the mutants' altered function with respect to membrane conductance and Na^+ sensitivity. The hDAT constructs were expressed in *Xenopus* oocytes to investigate if heightened membrane potential would explain the efflux characteristics of T62D-hDAT. In the absence of substrate, all constructs displayed identical resting membrane potentials. Substrate-induced inward currents were present in oocytes expressing WT- and T62A-hDAT but not T62D-hDAT suggesting bidirectional, equal ion flow through T62D-hDAT. Utilization of the fluorescent DAT substrate, ASP^+, revealed that T62D-hDAT accumulates substrate in HEK-293 cells when the substrate is not subject to efflux. Extracellular sodium (Na^+_e) replacement was used to evaluate sodium gradient requirements for DAT transport functions. The EC_{50} for Na^+_e stimulation of [^{3}H]DA uptake was identical in all constructs expressed in HEK-293 cells. As expected, decreasing $[Na^+]_e$ stimulated [^{3}H]DA efflux in WT- and T62A-hDAT cells. Conversely, the elevated [^{3}H]DA efflux in T62D-hDAT cells was independent of Na^+_e and commensurate with [^{3}H]DA efflux attained in WT-hDAT cells either by removal of Na^+_e or by application of AMPH. We conclude that T62D-hDAT represents an efflux-willing, Na^+-primed orientation—possibly representing an experimental model of the conformational impact of AMPH exposure to hDAT.

Molecular Pharmacology Fast Forward. Published on April 21, 2014 as DOI: 10.1124/mol.114.091926
This article has not been copyedited and formatted. The final version may differ from this version.

INTRODUCTION

The dopamine transporter (DAT) has a critical role in the regulation of dopamine (DA) neurotransmission due to its primary function of taking up released DA from the extracellular space back into the presynaptic nerve terminal. DAT is additionally the site of action for therapeutic and abused psychostimulants such as methylphenidate, amphetamine (AMPH), and cocaine (Levi and Raiteri, 1993; Leviel, 2011). AMPH is a competitive DAT substrate that, upon translocation into the terminal, is reported to release DA from synaptic vesicles, induce reverse transport, and subsequently increase extracellular DA (Sulzer et al., 2005).

The DAT is a member of the SLC6 family of transporters that require sodium and chloride ions for substrate translocation. The electrochemical gradient of Na^+ provides the energy required to move substrate through the transporter against its concentration gradient (Chen et al., 2004b; Hahn and Blakely, 2007). The alternate access model is the common paradigm for the translocation of neurotransmitter and co-transported ions (Jardetzky, 1966), where the transporter transitions between open-outward to open-inward orientations to move substrate from outside to inside the cell. Crystallization of the leucine transporter (LeuT), a bacterial SLC6 homolog (Krishnamurthy and Gouaux, 2012; Yamashita et al., 2005), provided considerable information about the Na^+ symporter structure and translocation mechanisms that further validate the alternate access model. DAT also generates unexpectedly large currents, and evidence exists for a channel mode of conduction (Carvelli et al., 2008; Carvelli et al., 2004; DeFelice and Goswami, 2007; Ingram et al., 2002). Elegant molecular modeling comparisons of LeuT to hDAT have identified fundamental transmembrane domains (TM) and amino acid residues involved in ligand binding and the extracellular to intracellular translocation of substrate (Shan et

Molecular Pharmacology Fast Forward. Published on April 21, 2014 as DOI: 10.1124/mol.114.091926
This article has not been copyedited and formatted. The final version may differ from this version.

al., 2011; Zhao et al., 2012; Zhao et al., 2010). However, the mechanisms regulating the binding of DA and co-transported ions during intracellular to extracellular transport are less understood.

The DAT N-terminus contains various serine and threonine residues that are important for the regulation of transporter activity (Foster et al., 2002) and AMPH-induced DA efflux (Foster et al., 2012; Khoshbouei et al., 2004). We investigated the putatively phosphorylated threonine residue within the highly conserved RETW sequence of the DAT N-terminus (Vaughan, 2004) for its role in the mechanisms of AMPH. The RETW sequence is juxtaposed to the TM1a segment (Yamashita et al., 2005), which is within a DAT region identified as the intracellular gating network (Kniazeff et al., 2008). Conservative (alanine, A) and non-conservative (aspartate, D) mutations were introduced at the Thr 62 residue, which also mimic a non-phosphorylated (T62A) and a phosphorylated (T62D) state (Guptaroy et al., 2009). As compared to WT-hDAT, T62D-hDAT HEK cells demonstrated a reduction in the uptake of [^{3}H]DA with a concomitant increase in the rate of basal DA release (Guptaroy et al., 2009). Moreover, T62D-hDAT was insensitive to AMPH. These functions were rescued when measured in the presence of zinc, which has been used to correct dysfunctions of other intracellular-favoring hDAT mutants (Loland et al., 2002; Meinild et al., 2004). The phenotype of T62A-hDAT cells was more similar to WT, with a reduction in both DA influx and AMPH-stimulated DA efflux. Additional studies revealed an enhanced affinity for DAT substrates in the T62 hDAT mutants (Guptaroy et al., 2011), particularly in the T62D-hDAT HEK cells. Enhanced substrate affinity can occur when the transition of substrate-bound transporter from the intracellular (inward) to extracellular (outward) orientation is kinetically favored (Chen et al., 2004a; Guptaroy et al., 2011; Guptaroy et al., 2009).

Molecular Pharmacology Fast Forward. Published on April 21, 2014 as DOI: 10.1124/mol.114.091926
This article has not been copyedited and formatted. The final version may differ from this version.

In this study we used the T62D-hDAT to further investigate the influence of transporter orientation on the membrane potential and the requirements of Na^+ in DAT functions. We examined if the elevated basal DA efflux measured in T62D-hDAT HEK cells could be attributed to 1) poor intracellular accumulation of substrate; 2) an intrinsic depolarization of the cell membrane; or 3) a modification in requirement for the Na^+ gradient. These hypotheses were tested using a combination of electrophysiology measurements in *Xenopus* oocytes and radioligand and fluorescent microscopy techniques in heterologous cells. The results from these experiments strengthened the conclusion that T62D-hDAT partitions in a conformation that represents an inward-favorable 'Na^+-primed' state able to maximize DA efflux.

Molecular Pharmacology Fast Forward. Published on April 21, 2014 as DOI: 10.1124/mol.114.091926
This article has not been copyedited and formatted. The final version may differ from this version.

MATERIALS AND METHODS

Construction and Expression of WT and Thr62 hDAT Mutants in Xenopus Oocytes

Restriction enzyme sites for 5' NotI and 3' XbaI were added to the flag-tagged WT and Thr62 hDAT mutant DNA constructs (Guptaroy et al., 2009) and subcloned into the pSGEM *Xenopus* oocyte expression vector. After linearization of the plasmid with SbfHI-HF digestion (New England BioLabs Inc., Ipswich, MA), capped RNA (cRNA) was prepared according to protocol with the mMessage mMachine T7 kit (Ambion Inc., Ausin, TX). *Xenopus* oocytes preparation was described previously (Solis et al., 2012). Stage IV-V oocytes were microinjected with 25 nl water or 25 ng (1ng/nl) hDAT cRNA using a Nanoject autoinjector (Drummond Scientific, Broomall, PA). Oocytes were incubated at 18° C in SuperBarth's solution, pH 7.4 [in mM: 88 NaCl, 1 KCl, 0.33 $Ca(NO_3)_2 \cdot 4H_2O$, 0.41 $CaCl_2 \cdot 2H_2O$, 1 $MgSO_4 \cdot 7H_2O$, 2.4 $NaHCO_3$, 10 HEPES, 1 Na-Pyruvate, and 50 mg/ml gentamicin] for 4-8 days before electrophysiology recordings.

Electrophysiology Measurements in Xenopus Oocytes Expressing WT and Thr 62 Mutant hDAT

Whole-cell currents or membrane potentials were measured by two-electrode voltage clamp techniques using a GeneClamp 500 (Molecular Devices, Palo Alto, CA). A 16-bit A/D converter (Digidata 1322A, Molecular Devices) interfaced to a PC running Clampex 10 (Molecular Devices) was used to control membrane voltage and acquire data. Microelectrodes were pulled using a programmable puller (Model P-87, Sutter Instrument, Novato, CA) to a resistance of 1.0-5.0 MΩ when filled with 3.0 M KCl electrode solution. Unless otherwise noted, oocytes were voltage clamped at -60 mV. Current was recorded continuously or with a step-voltage protocol.

Molecular Pharmacology Fast Forward. Published on April 21, 2014 as DOI: 10.1124/mol.114.091926
This article has not been copyedited and formatted. The final version may differ from this version.

The perfusion solutions were changed by a gravity-driven perfusion system at a rate of 1 ml/min. Oocytes were bathed/perfused in the HEPES-buffered solution ND96 [in mM: 96.0 NaCl, 2.0 KCl, 1.0 $MgCl_2$, 1.8 $CaCl_2$, and 5.0 HEPES-NaOH, pH 7.5]. All experiments were performed at room temperature (22–24°C).

Expression and Maintenance of WT and Thr62 Mutant hDAT HEK Cells

Wildtype, T62A, and T62D mutant human dopamine transporter (hDAT) were cloned and stably expressed in human embryonic kidney 293-T (HEK) cells as previously described (Guptaroy et al., 2009). Parental and hDAT HEK cells were maintained in high glucose Dulbecco's modified Eagle's medium supplemented with 10% fetal bovine serum and 1% penicillin/streptomycin at 37° C and 5% CO_2. All experiments utilizing hDAT HEK cells were performed with intact, attached cells at room temperature.

Measurement and Analysis of ASP^+ Accumulation with Live Cell Confocal Microscopy

Accumulation of the fluorescent substrate ASP^+ [4-(4-(dimethylamino)styryl)-N-methylpyridinium] (Molecular Probes, Eugene, OR) was measured with confocal imaging in live HEK cells (Schwartz et al., 2003; Zapata et al., 2007) expressing WT and Thr 62 mutant hDATs. Cells were plated on poly-D-lysine (PDL) coated, 35 mm glass bottom MatTek culture dishes (MatTek, Ashland, MA) at a density of 300,000-500,000 cells per dish 1 day prior to imaging. The culture media was aspirated and cells were washed twice in normal Krebs Ringer's HEPES (KRH) buffer, pH 7.4 [in mM: 125 NaCl, 4.8 KCl, 1.2 KH_2PO_4, 1.3 $CaCl{\bullet}2H_2O$, 1.2 $MgSO_4{\cdot}7H_2O$, 5.6 glucose, and 25 HEPES] containing 50 µM of pargyline (MAO inhibitor), 1 mM tropolone (COMT inhibitor), and 50 µM ascorbic acid (DA antioxidant) (Sigma, St. Louis, MO). Cells were incubated at 37° C in 2 ml of 5 µg/ml Hoechst nuclear stain (Molecular

Molecular Pharmacology Fast Forward. Published on April 21, 2014 as DOI: 10.1124/mol.114.091926
This article has not been copyedited and formatted. The final version may differ from this version.

Probes) for 30 min. Then cells were washed three times quickly and then twice more for 5 min each under light protection with gentle rocking. Plates were mounted on a Nikon A1R (Nikon Instruments, Inc., Melville, NY) confocal microscope with a 60x1.4 numerical aperture oil objective. Cell boundaries were confirmed with a differential interference contrast (DIC) image. Images were gathered 1 µm beyond the cell center, determined by the nuclear stain, to increase the accumulation measured within the cytosolic space. A test plate of WT-hDAT HEK cells was used to set the levels for intensity, brightness, and contrast for minimal saturation of the fluorescent signal of each laser channel. These microscope settings were not adjusted during the image acquisition of experiment plates. The Hoechst stain was excited with a UV laser at 405 nm and emission measured between 425-475 nm. ASP^+ was excited using the Cy3.5 laser with excitation at 561 nm and emission at 570-620 nm. Images were acquired at room temperature with a time scan every 10 sec for 3 min. ASP^+ (2 µM, 2 ml) was carefully added to the cells after the first 10 sec acquisition. The optical density (OD) within whole cell regions was quantified using ImageJ software (National Institutes of Health). Data are expressed as the OD measured within the cell across time. By the end of image acquisition (3 min), the background fluorescence in parental HEK cells was around 60% of the ASP^+ fluorescent signal in HEK cells expressing WT or Thr 62 mutant hDATs.

ASP^+ Competition of Radiolabeled Dopamine and WIN 35,428

Radioligand competition experiments were similar to assays described previously (Guptaroy et al., 2011; Guptaroy et al., 2009). Cells were seeded onto 24-well plates at a density of 200,000 cells per well 1 day before the experiment. Uptake of 10 nM [^{3}H]DA (specific activity 46 Ci/mmol) for 3 min or displacement of [^{3}H]WIN 35,438 (specific activity 85 Ci/mmol) binding for 30 min (Perkin Elmer Waltham, MA) were measured at room temperature with ASP^+ at

Molecular Pharmacology Fast Forward. Published on April 21, 2014 as DOI: 10.1124/mol.114.091926
This article has not been copyedited and formatted. The final version may differ from this version.

concentrations ranging from 0 to 1 mM (prepared in KRH buffer containing 10 % DMSO). Non-specific [^{3}H]DA uptake or [^{3}H]WIN 35,438 binding was determined in the presence of 100 µM cocaine or 5 µM GBR-12935, respectively, following a 10 minute preincubation with the inhibitor alone. At the end of the assay, cells were washed 4 times in ice cold phosphate buffered saline (PBS) then lysed in 0.25 ml 1% SDS. Radioactivity was measured in 5 ml of Scintiverse cocktail (Fisher Scientific, Waltham, MA) using a Beckman LS5801 scintillation counter (Fullerton, CA).

Extracellular Sodium Substitution

For experiments involving changing concentrations of extracellular sodium, NaCl in the KRH buffer was replaced with corresponding concentrations of N-methyl-D-glucamine chloride (NMDG-Cl). [^{3}H]DA uptake was measured as described above with varying levels of extracellular sodium (Na^+_e). Assay buffer with 0, 10, 30, 50, 100 and 125 mM NaCl contained 125, 115, 95, 75, 25, and 0 mM of NMDG-Cl, respectively. Maximum uptake was obtained in the normal 125 mM NaCl condition for all constructs.

For DA efflux experiments, cells were preloaded with 0.5 µM DA (containing 15 nM [^{3}H]DA) in normal KRH. After washing, 0.25 ml of fresh Na^+-substituted KRH was collected and replaced for 15 min to evaluate the baseline DA efflux. The effect of Na^+_e on AMPH-induced DA release was determined after a 5 min application of 10 µM AMPH, followed by collection of an additional 5 min aliquot at 20 min. At the end of the assay, cells were solubilized to measure the final amount of DA remaining inside of the cells after efflux. Total [^{3}H]DA after preloading was calculated as the sum of radioactivity in all efflux fractions and final intracellular DA. Basal DA efflux was calculated as a percentage of the calculated total [^{3}H]DA. AMPH-induced [^{3}H]DA

Molecular Pharmacology Fast Forward. Published on April 21, 2014 as DOI: 10.1124/mol.114.091926
This article has not been copyedited and formatted. The final version may differ from this version.

efflux was calculated as a percentage of the total [^{3}H]DA inside the cell prior to the AMPH treatment.

Statistical Analysis

The electrophysiological data were analyzed with clampfit 10 (Molecular Devices, Palo Alto, CA) and Origin 8 (OriginLab, Northampton, MA). Statistical differences were determined by 1-way analysis of variance (ANOVA) with Tukey's multiple comparisons test or unpaired *t*-test with Welch's correction using GraphPad Prism 6 software (San Diego, CA). Dose-response curves were analyzed with GraphPad Prism 6 software to determine the IC_{50} and EC_{50} values for [^{3}H]DA uptake competition by nonlinear regression analyses. Statistical differences were compared between constructs testing the null hypothesis of the parameter being the same between all data sets. A rejection of the null hypothesis indicated a statistical difference between the comparisons, where the p value was below 0.05. Values are provided ± standard error of the mean (s.e.m.) along with the 95% confidence intervals. Statistical differences for ASP^+ accumulation between cell types were determined by 2-way ANOVA with Tukey's multiple comparisons test at each time point.

Molecular Pharmacology Fast Forward. Published on April 21, 2014 as DOI: 10.1124/mol.114.091926
This article has not been copyedited and formatted. The final version may differ from this version.

RESULTS

Electrophysiological properties of hDAT mutants. DAT is an electrogenic transporter and current through the transporter in excess of the fixed stoichiometry of 1 Cl^-:2 Na^+:DA^+ has been detected (Sonders et al., 1997). Moreover, DAT-mediated DA efflux is greater at depolarized potentials (Khoshbouei et al., 2003). We posited that the changes in uptake and efflux of DA in the T62 hDAT mutants (Guptaroy et al., 2011) could correspond to altered electrophysiological properties. Therefore, we conducted electrophysiological studies of the hDAT and T62 hDAT mutants to supplement or disprove this hypothesis. The cRNAs for the mutants were transfected into *Xenopus* oocytes because transporter-mediated currents are large in these cells and much easier to measure than in cultured cells.

Xenopus oocytes were injected with equal amounts of hDAT cRNA for the three constructs. The DAT expression was confirmed by [^{3}H]DA uptake assays in 5 individual oocytes. DA uptake in hDAT-expressing oocytes was approximately 40% greater than in control water-injected oocytes 4 days after cRNA injections (data not shown). The resting membrane potentials (RMP) were measured in oocytes expressing the transporters and are summarized in Figure 1. The RMP in control oocytes was approximately -40 mV (-41.5 ± 2.6 mV). Expression of WT-, T62A-, or T62D-hDAT caused significant depolarization of the RMP to approximately -25 mV (WT-hDAT, -25.3 ±1.5 mV; T62A-hDAT, -27.0 ±1.4 mV; and T62D-hDAT, -24.3 ± 1.1 mV), which was statistically different from the RMP in control oocytes (Control vs. WT and T62D, $p < 0.0001$; Control vs T62A, $p = 0.0014$). However, the level of depolarization induced by T62A- or T62D-hDAT expression in the oocytes was not different from that of WT-hDAT oocytes. The well-characterized leak current present in DAT in the absence of substrate (Sonders et al., 1997)

Molecular Pharmacology Fast Forward. Published on April 21, 2014 as DOI: 10.1124/mol.114.091926
This article has not been copyedited and formatted. The final version may differ from this version.

is likely accountable for the depolarization of the oocyte. Therefore, the baseline current passing through the transporter in the absence of substrate is not affected by the Thr 62 mutations.

DAT substrates, such as DA and AMPH, induce inward currents that are primarily attributed to an inward flux of Na^+ ions (Sonders et al., 1997). The substrate-induced currents in oocytes expressing WT-, T62A-, and T62D-hDAT were recorded with a holding potential of -60 mV. Representative trace recordings from oocytes are shown in Figure 2A and the changes in accumulated current in WT-, T62A-, and T62D-hDAT oocytes held at -60 mV are shown in Figure 2B. Currents were measured after the application of 10 μM DA for 1 minute. DA produced inward currents in oocytes expressing WT-hDAT and T62A-hDAT that were absent in control oocytes lacking the transporter. The fast phase of the inward current lasted less than 10s followed by a slow recovery phase. The change in current before and after DA application was -6.60 ± 1.53 nA in WT-hDAT, -3.85 ± 0.38 nA in T62A-hDAT, and -0.34 ± 0.30 in T62D-hDAT. Negligible current was measured in response to DA in the T62D-hDAT oocytes. These results correspond with our previous reports of a substantial reduction in the V_{max} for [^{3}H]DA uptake in T62A-hDAT HEK293 cells as compared to WT-hDAT HEK293 cells (Guptaroy et al., 2009). Similar results were recorded with the application of AMPH (data not shown). Membrane conductance was next measured with a step voltage protocol and the current difference is plotted in Figure 3. While membrane conductance was observed with DA application to WT- and T62A-hDAT oocytes (Figures 2A and 2C), the I-V curves confirmed there was no change in conductance with the application of DA (Figure 3C) or AMPH (data not shown) in T62D-hDAT oocytes. T62D-hDAT is expressed at the oocyte plasma membrane since [^{3}H]DA uptake experiments from different oocytes confirmed expression and function of T62D-hDAT. Zinc has been used to improve transport in T62D-hDAT HEK293 cells (Guptaroy et al., 2011; Guptaroy

Molecular Pharmacology Fast Forward. Published on April 21, 2014 as DOI: 10.1124/mol.114.091926
This article has not been copyedited and formatted. The final version may differ from this version.

et al., 2009) and other uptake-defective DAT mutant transporters (Chen et al., 2004a; Loland et al., 2002). Binding of zinc stabilizes a conformation of DAT that increases chloride conductance (Loland et al., 2002; Meinild et al., 2004). The use of zinc was employed to further validate the function of T62D-hDAT expressing oocytes. Co-application of DA and 2 μM $ZnCl_2$ after treatment of DA alone in the same T62D-hDAT oocyte produced a measurable substrate-induced current (Figure 2A). Although Zn^{2+} *per se* induced small inward currents in each transcript, as seen in Figures 2B and 3, it significantly potentiated the DA-induced inward current measured at -60 mV in the hDAT oocytes (comparison of values DA ± zinc: WT-hDAT, $p = 0.02$; T62A-hDAT, $p < 0.0001$; and T62D-hDAT, $p = 0.0003$). These data not only provided functional evidence for the membrane expression of T62D-hDAT, but demonstrated that the defective gating of the T62D-hDAT mutant could be partially rescued by zinc. As the holding potential became higher than the reversal potential, outward currents in all the hDAT constructs were similar with the application of zinc alone or in combination with DA. Outward currents at depolarizing potentials were not observed without application of zinc (Figure 3).

Affinity and Accumulation of the Fluorescent Substrate, ASP^+ in WT and Thr hDAT Mutant HEK Cells. In previous studies (Guptaroy et al., 2009), we found that T62D-hDAT demonstrated high affinity, but very low V_{max} for [^{3}H]DA uptake with high basal efflux. We postulated that substrate would not accumulate intracellularly due to accelerated outward transport. K_m and V_{max} values for [^{3}H]DA uptake for T62A-hDAT were intermediate between T62D-hDAT and WT (Guptaroy et al., 2009). To test this explanation, we conducted uptake experiments with the three constructs expressed in HEK cells using the fluorescent monoamine transporter substrate, 4-(4-(dimethylamino)styryl)-*N*-methylpyridinium (ASP^+). ASP^+ is structurally similar to the dopaminergic neurotoxin, 1-methyl-4-phenylpyridinium (MPP^+).

Molecular Pharmacology Fast Forward. Published on April 21, 2014 as DOI: 10.1124/mol.114.091926
This article has not been copyedited and formatted. The final version may differ from this version.

ASP^+ is taken up normally through the transporters but due to intracellular binding to mitochondria, is not available for efflux (Schwartz et al., 2003).

Uptake and binding of the ASP^+ substrate to the WT and Thr62 mutant hDAT HEK constructs were confirmed with radioligand competition assays. Dose response curves for ASP^+ competition of [^{3}H]DA uptake (Figure 4A) and displacement of the cocaine analog [^{3}H]WIN 35,428 (Figure 4B) did not differ among WT and Thr 62 hDAT mutant cell lines. The IC_{50} values (μM) [with 95% confidence intervals] for ASP^+ competition of [^{3}H]DA uptake were 11.95 [8.87-16.1] in WT-, 17.60 [10.6-29.2] in T62A-, and 12.08 [10.3-14.1] in T62D-hDAT HEK cells (Figure 4A). ASP^+ inhibited [^{3}H]WIN 35,428 binding with IC_{50} (μM) values of 11.95 [8.87-16.1] in WT-, 18.6 [10.6-29.2] in T62A-, and 12.1 [10.3-14.1] in T62D-hDAT HEK cells (Figure 4B).

Using fluorescence microscopy, we measured uptake of ASP^+ (Figure 5). There was a low level of background fluorescence prior to the addition of ASP^+ which did not differ among cell types. However, the fluorescence intensity increased with time after cells containing the DAT constructs were exposed to 2 μM of ASP^+. Representative confocal images prior to (time 0) and after (3 min) ASP^+ addition are shown for WT-, T62A-, T62D-hDAT, and parental HEK 293T cells in Figure 5A-D. The full time course of intracellular ASP^+ accumulation in each cell type is shown in Figure 5E. There was no difference in ASP^+ uptake among WT-, T62A-, and T62D-hDAT cells, but ASP^+ uptake in the three DAT-containing cell lines was significantly different from that in parental HEK cells at all time points ($p < 0.0001$ for genotype, $F(3, 558) = 54.06$; time $F(19, 10602) = 2360$, and interaction between genotype and time, $F(57, 10602) = 31.37$). The linear rate of ASP^+ uptake in O.D. units/sec during the first 30 seconds [95% CI] was 0.123 [0.109-0.137] for WT-hDAT, 0.110 [0.096-0.125] for T62A-hDAT, and 0.103 [0.089-

Molecular Pharmacology Fast Forward. Published on April 21, 2014 as DOI: 10.1124/mol.114.091926
This article has not been copyedited and formatted. The final version may differ from this version.

0.116] for T62D-hDAT versus 0.043 [0.032-0.053] in parental HEK cells. The uptake rate in the parental HEK cells significantly differed from the cells containing the three DAT constructs at $p < 0.0001$, $F=29.7246$, $DF_n = 3$, $DF_d = 2240$. To demonstrate that the results with uptake of ASP^+ were due to the T62D mutation and not the substrate itself, we performed uptake and efflux experiments with $[^3H]MPP^+$ in WT- and T62D-hDAT cells. $[^3H]MPP^+$ is structurally similar to ASP^+ but is readily subject to reverse transport through DAT. Results are highly similar to those using $[^3H]DA$ (Guptaroy et al., 2009). The uptake of $[^3H]MPP^+$ in pmol/min/mg protein with [95% CI] was 260 [222-297] in WT-hDAT cells versus 8.4 [5.8-10.9] in T62D-hDAT cells ($p < 0.0005$, $F = 45.7$ (1,6) for an experiment performed in triplicate. The linear rate of $[^3H]MPP^+$ efflux, in pmol $[^3H]MPP^+/\mu M$ intracellular $[^3H]MPP^+$ [95% CI], is 6.5 [4.3-8.5] for WT cells and 24.9 [22.5-27.3] for T62D-hDAT cells ($p = 0.00067$, $F = 91.3$ (1,4)).

Differential Sodium Requirements for DA Uptake versus Efflux in T62D-hDAT Mutants. Given our findings of identical intracellular ASP^+ retention among the DAT constructs despite differences in substrate-induced membrane conductance, we next explored the effect of Na^+ on the function of T62D-hDAT as compared to the other constructs. To determine whether the Thr 62 mutations would alter the Na^+ requirements for hDAT function, we measured $[^3H]DA$ uptake and efflux in WT-, T62A-, and T62D-hDAT HEK cells while varying the extracellular concentrations of Na^+ [Na^+_e]. NaCl was replaced with NMDG-Cl to maintain osmolarity of the cells. In all cell lines, there was very little uptake of $[^3H]DA$ with complete NMDG-Cl substitution (0 mM Na^+_e) but $[^3H]DA$ uptake increased identically in all three cell lines as the [Na^+_e] rose. There was no statistical difference between the EC_{50} (mM) [95% CI] values for Na^+ stimulation of $[^3H]DA$ uptake in WT- 39.6 [26.7-58.5], T62A- 40. 5 [29.7-55.1], or T62D-hDAT HEK cells 58.7 [39.4-87.6] (Figure 6).

Molecular Pharmacology Fast Forward. Published on April 21, 2014 as DOI: 10.1124/mol.114.091926
This article has not been copyedited and formatted. The final version may differ from this version.

Outward transport through DAT demonstrates an inverse dependence on Na^+_e as compared to inward transport. Removal or lowering of extracellular Na^+ stimulates substrate efflux in cells expressing monoamine transporters (Pifl et al., 1997; Pifl and Singer, 1999) or brain tissue preparations (Liang and Rutledge, 1982; Raiteri et al., 1979) by shifting the internal Na^+ gradient to favor reversal of the transporter. Previously we reported that T62D-hDAT had an elevated basal leak of [^{3}H]DA, which exceeded that of WT at physiological levels of Na^+_e (Guptaroy et al., 2009). Here, the behavior of the basal and AMPH-stimulated efflux as a function of Na^+_e was examined.

WT-hDAT HEK cells showed the expected elevation in basal [^{3}H]DA efflux upon removal of Na^+_e and the elevation was maintained throughout the 15 min incubation period (Figure 7A, open bars). The baseline efflux significantly decreases as [Na^+_e] progresses from 0 mM to 10 mM, 50 mM and 125 mM (Figure 7A, clear, checkered, gray, and black bars, please see figure legend for statistics for varied Na^+_e at individual time points). This same pattern recurred at the 10 min and 15 min time points (Figure 7A, checkered, gray, and black bars). In a 2-way ANOVA, there was a main effect of time ($p < 0.01$ ($F_{(3, 56)} = 8.043$)) and a significant interaction between [Na^+_e] and time ($p < 0.0001$ ($F_{(9, 56)} = 12.80$)) with no main effect of [Na^+_e] ($p = 0.08$, $F_{(3, 56)} = 3.24$). Significant stimulation of efflux by 10 μM AMPH above the corresponding baseline is only evident at 50 mM Na^+_e ($p < 0.05$, *post hoc* Tukey's) and 125 mM Na^+_e ($p < 0.0001$, *post hoc* Tukey's) (Figure 7A, 20 min). On the contrary, at 0 mM Na^+_e, 10 μM AMPH significantly decreased basal [^{3}H]DA efflux from corresponding baseline ($p < 0.05$, *post hoc* Tukey's).

The pattern was similar but less pronounced in T62A-hDAT HEK cells even though the degree of [^{3}H]DA efflux was slightly lower than in WT (Figure 7B). By 2-way ANOVA, there was a significant effect of time ($p < 0.01$, ($F_{(3, 46)} = 5.391$)), and interaction of [Na^+_e] and time (p

Molecular Pharmacology Fast Forward. Published on April 21, 2014 as DOI: 10.1124/mol.114.091926
This article has not been copyedited and formatted. The final version may differ from this version.

<0.0001, $F_{(9, 46)} = 6.289$), but no significant effect of [Na^+_e] (p=0.0.476, $F_{(3, 46)} = 0.842$). The enhancement of [3H]DA efflux elicited by low Na^+_e was most evident at the 5 min time point. For clarity, statistical results for individual time periods are given in the legend to Figure 7. As in WT-hDAT, AMPH significantly increased [^{3}H]DA efflux only at 50 mM and 125 mM Na^+_e. There was a tendency for AMPH to decrease [^{3}H]DA efflux at 0 mM Na^+_e as compared to the 15 min baseline efflux at 0 mM Na^+_e ; however, the difference was not statistically significant.

In T62D-hDAT HEK cells (Figure 7C), there visually appeared to be a run-down in [^{3}H]DA efflux as time progressed, but it was independent of Na^+_e. There was a significant effect of time by 2-way ANOVA ($p < 0.0001$, $F_{(3, 51)} = 25.07$) but no interaction with time and [Na^+_e] and no main effect of [Na^+_e]. The decline in [^{3}H]DA efflux was not due to a loss of intracellular [^{3}H]DA since 70% - 80% of the [^{3}H]DA originally taken up was still inside the cell after 20 min. AMPH does not induce [^{3}H]DA efflux at any [Na^+_e] in the T62D-hDAT mutant (Figure 7C). All values at the 20 min time point where AMPH was present were significantly different from values for 0 mM Na^+_e at 5 min and 10 min ($p < 0.05$ for both time points) but not 15 min when all possible comparisons were made.

In order to better visualize the similarities or differences between T62D- and WT-hDAT, data for only these two constructs at 0 mM and 125 mM Na^+_e were graphed (Figure 7D). In a general linear model 3-way ANOVA, there was a significant effect of *time x cell type* (F=10.277, df=3, p=0.0001), a significant *time x sodium interaction* (F=14.951, df=3, p = 0.0001) and a significant *time x cell type x sodium interaction* (F=10.190, df=3, p = 0.0001). There was no significant *cell type x sodium interaction* (p = 0.5). At the initial 5 min time point, [^{3}H]DA efflux in WT-hDAT was significantly elevated at 0 mM Na^+_e versus 125 mM Na^+_e (p = 0.001). Conversely, the level of [^{3}H]DA efflux is identical for T62D-hDAT at 0 and 125 mM Na^+_e (p = 0.647) and for WT at 0

Molecular Pharmacology Fast Forward. Published on April 21, 2014 as DOI: 10.1124/mol.114.091926
This article has not been copyedited and formatted. The final version may differ from this version.

mM Na^+_e ($p = 0.612$). Therefore, removal of Na^+_e transformed WT-hDAT into an efflux-favoring conformation that is simulated by T62D-hDAT independently of Na^+_e. [^{3}H]DA efflux in WT-hDAT remained stable between 5 and 15 min whether at 0 mM Na^+_e or 125 mM Na^+_e. On the contrary, baseline [^{3}H]DA efflux in T62D-hDAT at both 0 mM and 125 mM Na^+_e began to decline within the first 10 min and the decrease was statistically significant at 15 min (see statistical values in legend for Figure 7D). This decline continued even during the 5 min incubation with 10 μM AMPH (20 min point). The baseline efflux of [^{3}H]DA at 5 min in WT-hDAT at 0 mM Na^+_e was not statistically different from that elicited by 5 min of AMPH at 125 mm Na^+_e or the initial 5 min Na^+_e-independent efflux observed in T62D-hDAT. From all the aforementioned interactions, we reasoned the T62D-hDAT mutation produces a Na^+-primed state of the transporter that readily releases DA.

[^{3}H]DA efflux was sensitive to inhibition by 100 μM cocaine in all three DAT constructs. The fractional efflux of [^{3}H]DA in the presence of 100 μM cocaine was constant within each construct independent of time and [Na^+_e]. Fractional [^{3}H]DA release in the presence of 100 μM cocaine is 6.4 ± 0.1 for WT, 7.3 ± 0.6 for T62A-hDAT, and 4.9 ± 0.2 for T62D-hDAT (n=4 each cell type, for all [Na^+_e]).

Molecular Pharmacology Fast Forward. Published on April 21, 2014 as DOI: 10.1124/mol.114.091926
This article has not been copyedited and formatted. The final version may differ from this version.

DISCUSSION

This study provides evidence of differential regulation of DA uptake versus efflux functions in T62D-hDAT mutant; the disparity is accounted for by altered Na^+ regulation. A number of DAT mutants with restricted substrate influx have been identified, but few have been characterized for both forward and reverse transport. The DAT Thr 62 mutations are poised to provide key information concerning transporter conformational transitions. Despite striking differences in uptake and efflux behaviors for [^{3}H]DA, we found T62D-hDAT exhibited some characteristics identical to WT and to T62A-hDAT: membrane depolarization when expressed in *Xenopus* oocytes, uptake of the substrate ASP^+ when efflux was not a factor, and Na^+ concentration dependence of DA uptake. Despite its predilection to leak DA, T62D-hDAT assumes a conformation that confers normal uptake function and extracellular Na^+ binding. While WT transporter requires Na^+ to reverse and expel DA, T62D-hDAT does not. T62D-hDAT appears to mimic a substrate- and Na^+-elicited conformation that normally permits reverse transport. The dual demonstration of normal DA uptake but constitutive efflux suggests T62D-hDAT is not fixed in position. Instead, T62D-hDAT may rapidly transition among the conformations for influx and efflux in sodium dependent and independent fashions, respectively.

Networks of molecular interactions drive substrate movement and transporter conformations. Thr 62 is within a prime location to affect transporter orientation due to its proximity to transmembrane (TM) 1a, which forms part of the permeation pathway (Shan et al., 2011; Yamashita et al., 2005). TM1a is within an intracellular gating network (Kniazeff et al., 2008) that regulates DAT conformational transitions (Shan et al., 2011). Several DAT mutants, including T62D-hDAT, demonstrate particularly low DA inward transport. The D345N-hDAT

Molecular Pharmacology Fast Forward. Published on April 21, 2014 as DOI: 10.1124/mol.114.091926
This article has not been copyedited and formatted. The final version may differ from this version.

and Y335A-hDAT (Chen et al., 2004a; Loland et al., 2002), have been referred to as 'inward-facing' meaning the transporter prefers a conformation in which the intracellular-facing gate is more accessible than the extracellular-facing gate. Intracellular interactions of these mutants have been characterized lending credence to the designation of 'inward-facing' (Loland et al., 2004). We apply a similar description for the T62D-hDAT mutant (Guptaroy et al., 2009). Our study demonstrates that conformational transitions of the mutant are more complex than a simple delineation of inward and outward facing.

The fluorescent substrate, ASP^+, permitted interrogation of whether the Thr 62 hDAT mutations truly disrupt the influx of substrate and, by inference, its intracellular retention. ASP^+ is well characterized as a substrate for both DAT and NET (Schwartz et al., 2003). Once inside of cells, ASP^+ sequesters within mitochondria (Schwartz et al., 2003) and, as a non-catechol substrate, will not bind to the cytoplasmic side of the transporter to undergo outward transport (Liang et al., 2009). Identical ASP^+ accumulation in T62D- and WT-hDAT points to normal (outward to inward) translocation in T62D-hDAT. Therefore, the extremely low V_{max} of [^{3}H]DA in T62D-hDAT cells (Guptaroy et al., 2009) was due to continuous intracellular rebinding of [^{3}H]DA and its outward transport. This distinguishes T62D-hDAT from other DAT mutants characterized as inward facing (Chen et al., 2004a; Loland et al., 2002). The data also demonstrate T62A-hDAT takes up substrate identically to WT despite its V_{max} for DA uptake being about one-half of WT hDAT (Guptaroy et al., 2009). Both influx and efflux functions of T62A-hDAT are compromised, but to a lower extent than T62D-hDAT (Guptaroy et al., 2009). The T62D-hDAT mutant shares similar characteristics to A559V-hDAT, a variant isolated from 2 male siblings with ADHD (Mazei-Robison et al., 2008) and T356M-hDAT, a *de novo* mutation associated with autism spectrum disorder (Hamilton et al., 2013). Like T62D-, A559V- and T356M-hDAT

Molecular Pharmacology Fast Forward. Published on April 21, 2014 as DOI: 10.1124/mol.114.091926
This article has not been copyedited and formatted. The final version may differ from this version.

exhibit elevated baseline leak of DA and inhibition of outward efflux by AMPH (Mazei-Robison et al., 2008; Hamilton et al., 2013). The diminution of DA efflux by DA in WT-hDAT under low Na^+_e conditions, as observed in our study, was also noted by Pifl and Singer (1999).

Measurement of DAT currents indicate greater quantities of ions travel across the membrane than predicted (Sonders et al., 1997) by the stoichiometric ratio of 1DA:2Na^+:1Cl^- (Rudnick, 1998). This implies a channel function of the transporter along with a substrate transport process. The similar depolarization exhibited in our DAT construct expressing oocytes is likely the result of a common, substrate-independent leak current (Sonders et al., 1997). Conversely, profound differences in current conductance in *Xenopus* oocytes expressing WT- and T62D-hDAT were found when measured with substrate. No net current was detected in response to either DA or AMPH in T62D-hDAT oocytes. Absence of ion movement through T62D-hDAT is unlikely because the mutant exhibits normal Na^+-dependent substrate uptake. A net ion flux was restored in T62D-hDAT by the addition of Zn^{2+}. Zinc rescues influx in DAT mutants presenting drastically reduced DA uptake, such as Y335A-hDAT (Meinild et al., 2004) or D345N-hDAT (Chen et al., 2004a), and T62D-hDAT (Guptaroy et al., 2009). Here, Zn^{2+} enabled current measurement in the T62D-hDAT. Despite this restoration, there are diverse Zn^{2+} effects on various DAT mutants characterized as 'inward-facing', reflecting structural and conformation differences amongst the mutants that result in low substrate uptake. For instance, Zn^{2+} partly restored AMPH-induced DA efflux in T62D-hDAT-HEK cells (Guptaroy et al., 2009) but not in D345N-hDAT-HEK cells (Chen et al., 2004a).

Na^+ is a key determinant for the function of co-transporters. The electrophysiological phenotypes of WT- and T62D-hDAT oocytes in the presence and absence of substrate suggested the T62D mutation may affect Na^+ transport requirements. The interpretation that Thr 62

Molecular Pharmacology Fast Forward. Published on April 21, 2014 as DOI: 10.1124/mol.114.091926
This article has not been copyedited and formatted. The final version may differ from this version.

mutations were primarily affecting transitions in the efflux pathway was strengthened by finding that the sodium requirement for DA influx was identical amongst the three DAT constructs. Reduction of the transmembrane Na^+ electrochemical gradient by either increasing intracellular Na^+ or reducing extracellular Na^+ inhibits neurotransmitter uptake but simultaneously promotes reverse transport (Erreger et al., 2008; Khoshbouei et al., 2003; Liang and Rutledge, 1982; Raiteri et al., 1979; Zhen et al., 2005) due to the build-up of Na^+ at the cytosolic face of the transporter (Liang and Rutledge, 1982; Raiteri et al., 1979). Khoshbouei et al. (2003) directly demonstrated this and proposed that AMPH-induced inward current increases intracellular Na^+ availability to DAT. T62D-hDAT, however, was insensitive to changes in the Na^+ electrochemical gradient such that reverse transport required no change in Na^+_e. This hints at the T62D-hDAT conformation existing in a Na^+-receptive orientation. Single molecule fluorescence resonance energy transfer imaging of the Na^+-symporter DAT homolog, LeuT, at TM1a revealed two distinguishable states of the transporter in the absence of Na^+, consistent with two distinct conformations of the intracellular gate (Zhao et al., 2010; Zhao et al., 2011). Addition of Na^+ or substrate decreased the transition frequency leading to preferential stabilization of an inward-closed state. Previous *in silico* modeling of T62D-hDAT in comparison to WT-hDAT indicated a disruption of a functionally important microenvironment involving binding of T62 to other residues at the intracellular side (Guptaroy et al., 2009) and within an intracellular gating network (Kniazeff et al., 2008). Therefore, the T62D mutation can sustain multiple conformations of DAT, or lead to rapid inter-conversions of these conformations, with respect to the status of the inward-facing gate near TM1a. One conformation would permit normal Na^+ binding and influx while another orientation mimics the intracellular Na^+-primed state normally achieved as a result of AMPH action. We previously demonstrated that the K_m for [^{3}H]DA at the

Molecular Pharmacology Fast Forward. Published on April 21, 2014 as DOI: 10.1124/mol.114.091926
This article has not been copyedited and formatted. The final version may differ from this version.

intracellular side of T62D-hDAT is significantly less than that of WT (Guptaroy et al., 2009). The Na^+-primed conformation of DAT readily rebinds DA, and it is unlikely that empty transporter returns to the surface. Thus, one of the conformations adopted by T62D-hDAT represents a Na^+-primed state that favors reverse transport.

The Na^+-sensitivity of other DAT mutants has not been routinely measured. The A559V-hDAT variant demonstrated an enhanced sensitivity but remained responsive to intracellular Na^+ (Mazei-Robison et al., 2008). T62D-hDAT was unresponsive to partial, indirect changes in the transmembrane Na^+ gradient via extracellular Na^+ substitution. Nonetheless, the similarities underscore the importance of the sodium gradient in maintaining conformational states of DAT.

This study revealed novel attributes of hDAT Thr 62 mutations, particularly in mutation of Thr 62 to aspartate. This mutation makes evident that DAT exists in conformations that exhibit normal substrate uptake with unregulated efflux. T62A-hDAT is a less severe mutation, showing reduced sensitivity to AMPH but not the overtly unregulated efflux attained by T62D-hDAT. T62D-hDAT binds Na^+ and transports DA inward normally, but has lost the capacity for intracellular Na^+ to stimulate shifts in transporter orientation. Taken together, our data place importance on the molecular interactions between residues involving Na^+ differentially influencing the efflux properties of the transporter. The T62D-hDAT and other transporter mutants can serve as informational experimental models for changes that occur to the transporter after exposure to AMPH.

Molecular Pharmacology Fast Forward. Published on April 21, 2014 as DOI: 10.1124/mol.114.091926
This article has not been copyedited and formatted. The final version may differ from this version.

Acknowledgments

We would like thank Dr. Asim Beg (University of Michigan) for the pSGEM oocyte construct and initial help with *Xenopus* oocyte studies. We are grateful to Dr. Samuel Straight at the Center for Live Cell Imaging for initial consultation and assistance with confocal image analysis. We also appreciate the statistical analyses of 3-way interactions provided by Felicia R. Webb at the University of Michigan. We acknowledge the University of Michigan Pharmacology Department confocal microscopy facility and the DNA Sequencing Core. Lastly, we would like to thank Sarah Mikelman for technical assistance.

Authorship Contributions

Participated in research design: Fraser, Chen, DeFelice, Gnegy

Conducted experiments: Fraser, Chen, Luderman, Stokes

Contributed new reagents or analytical tools: Fraser, Chen, Guptaroy, Beg

Performed data analysis: Fraser, Chen, DeFelice, Gnegy

Wrote or contributed to writing of the manuscript: Fraser, Chen, DeFelice, Gnegy

Molecular Pharmacology Fast Forward. Published on April 21, 2014 as DOI: 10.1124/mol.114.091926
This article has not been copyedited and formatted. The final version may differ from this version.

REFERENCES

Carvelli, L., Blakely, R.D., and DeFelice, L.J. (2008). Dopamine transporter/syntaxin 1A interactions regulate transporter channel activity and dopaminergic synaptic transmission. Proceedings of the National Academy of Sciences of the United States of America *105*, 14192-14197.

Carvelli, L., McDonald, P.W., Blakely, R.D., and Defelice, L.J. (2004). Dopamine transporters depolarize neurons by a channel mechanism. Proceedings of the National Academy of Sciences of the United States of America *101*, 16046-16051.

Chen, N., Rickey, J., Berfield, J.L., and Reith, M.E. (2004a). Aspartate 345 of the dopamine transporter is critical for conformational changes in substrate translocation and cocaine binding. The Journal of biological chemistry *279*, 5508-5519.

Chen, N.H., Reith, M.E., and Quick, M.W. (2004b). Synaptic uptake and beyond: the sodium- and chloride-dependent neurotransmitter transporter family SLC6. Pflugers Archiv : European journal of physiology *447*, 519-531.

DeFelice, L.J., and Goswami, T. (2007). Transporters as channels. Annual review of physiology *69*, 87-112.

Erreger, K., Grewer, C., Javitch, J.A., and Galli, A. (2008). Currents in response to rapid concentration jumps of amphetamine uncover novel aspects of human dopamine transporter function. J Neurosci *28*, 976-989.

Foster, J.D., Pananusorn, B., and Vaughan, R.A. (2002). Dopamine transporters are phosphorylated on N-terminal serines in rat striatum. The Journal of biological chemistry *277*, 25178-25186.

Foster, J.D., Yang, J.W., Moritz, A.E., Challasivakanaka, S., Smith, M.A., Holy, M., Wilebski, K., Sitte, H.H., and Vaughan, R.A. (2012). Dopamine transporter phosphorylation site threonine 53 regulates substrate reuptake and amphetamine-stimulated efflux. The Journal of biological chemistry *287*, 29702-29712.

Guptaroy, B., Fraser, R., Desai, A., Zhang, M., and Gnegy, M.E. (2011). Site-Directed Mutations near Transmembrane Domain 1 Alter Conformation and Function of Norepinephrine and Dopamine Transporters. Molecular pharmacology *79*, 520-532.

Guptaroy, B., Zhang, M., Bowton, E., Binda, F., Shi, L., Weinstein, H., Galli, A., Javitch, J.A., Neubig, R.R., and Gnegy, M.E. (2009). A juxtamembrane mutation in the N terminus of the dopamine transporter induces preference for an inward-facing conformation. Molecular pharmacology *75*, 514-524.

Hahn, M.K., and Blakely, R.D. (2007). The functional impact of SLC6 transporter genetic variation. Annual review of pharmacology and toxicology *47*, 401-441.

Hamilton, P.J., Campbell, N.G., Sharma, S., Erreger, K., Herborg Hansen, F., Saunders, C., Belovich, A.N., Consortium, N.A.A.S., Sahai, M.A., Cook, E.H., *et al.* (2013). De novo mutation in the dopamine transporter gene associates dopamine dysfunction with autism spectrum disorder. Molecular psychiatry *18*, 1315-1323.

Ingram, S.L., Prasad, B.M., and Amara, S.G. (2002). Dopamine transporter-mediated conductances increase excitability of midbrain dopamine neurons. Nature neuroscience *5*, 971-978.

Jardetzky, O. (1966). Simple allosteric model for membrane pumps. Nature *211*, 969-970.

Khoshbouei, H., Sen, N., Guptaroy, B., Johnson, L., Lund, D., Gnegy, M.E., Galli, A., and Javitch, J.A. (2004). N-terminal phosphorylation of the dopamine transporter is required for amphetamine-induced efflux. PLoS Biol *2*, E78.

Khoshbouei, H., Wang, H., Lechleiter, J.D., Javitch, J.A., and Galli, A. (2003). Amphetamine-induced dopamine efflux. A voltage-sensitive and intracellular Na+-dependent mechanism. The Journal of biological chemistry *278*, 12070-12077.

Kniazeff, J., Shi, L., Loland, C.J., Javitch, J.A., Weinstein, H., and Gether, U. (2008). An intracellular interaction network regulates conformational transitions in the dopamine transporter. The Journal of biological chemistry *283*, 17691-17701.

Krishnamurthy, H., and Gouaux, E. (2012). X-ray structures of LeuT in substrate-free outward-open and apo inward-open states. Nature *481*, 469-474.

Levi, G., and Raiteri, M. (1993). Carrier-mediated release of neurotransmitters. Trends in neurosciences *16*, 415-419.

Leviel, V. (2011). Dopamine release mediated by the dopamine transporter, facts and consequences. Journal of neurochemistry *118*, 475-489.

Liang, N.Y., and Rutledge, C.O. (1982). Evidence for carrier-mediated efflux of dopamine from corpus striatum. Biochem Pharmacol *31*, 2479-2484.

Liang, Y.J., Zhen, J., Chen, N., and Reith, M.E. (2009). Interaction of catechol and non-catechol substrates with externally or internally facing dopamine transporters. Journal of neurochemistry *109*, 981-994.

Loland, C.J., Granas, C., Javitch, J.A., and Gether, U. (2004). Identification of intracellular residues in the dopamine transporter critical for regulation of transporter conformation and cocaine binding. The Journal of biological chemistry *279*, 3228-3238.

Loland, C.J., Norregaard, L., Litman, T., and Gether, U. (2002). Generation of an activating Zn(2+) switch in the dopamine transporter: mutation of an intracellular tyrosine constitutively alters the conformational equilibrium of the transport cycle. Proceedings of the National Academy of Sciences of the United States of America *99*, 1683-1688.

Mazei-Robison, M.S., Bowton, E., Holy, M., Schmudermaier, M., Freissmuth, M., Sitte, H.H., Galli, A., and Blakely, R.D. (2008). Anomalous dopamine release associated with a human dopamine transporter coding variant. J Neurosci *28*, 7040-7046.

Meinild, A.K., Sitte, H.H., and Gether, U. (2004). Zinc potentiates an uncoupled anion conductance associated with the dopamine transporter. The Journal of biological chemistry *279*, 49671-49679.

Pifl, C., Agneter, E., Drobny, H., Reither, H., and Singer, E.A. (1997). Induction by low Na+ or Cl- of cocaine sensitive carrier-mediated efflux of amines from cells transfected with the cloned human catecholamine transporters. British journal of pharmacology *121*, 205-212.

Pifl, C., and Singer, E.A. (1999). Ion dependence of carrier-mediated release in dopamine or norepinephrine transporter-transfected cells questions the hypothesis of facilitated exchange diffusion. Molecular pharmacology *56*, 1047-1054.

Raiteri, M., Cerrito, F., Cervoni, A.M., and Levi, G. (1979). Dopamine can be released by two mechanisms differentially affected by the dopamine transport inhibitor nomifensine. The Journal of pharmacology and experimental therapeutics *208*, 195-202.

Rudnick, G. (1998). Ion-coupled neurotransmitter transport: thermodynamic vs. kinetic determinations of stoichiometry. Methods in enzymology *296*, 233-247.

Schwartz, J.W., Blakely, R.D., and DeFelice, L.J. (2003). Binding and transport in norepinephrine transporters. Real-time, spatially resolved analysis in single cells using a fluorescent substrate. The Journal of biological chemistry *278*, 9768-9777.

Shan, J., Javitch, J.A., Shi, L., and Weinstein, H. (2011). The substrate-driven transition to an inward-facing conformation in the functional mechanism of the dopamine transporter. PloS one *6*, e16350.

Solis, E., Jr., Zdravkovic, I., Tomlinson, I.D., Noskov, S.Y., Rosenthal, S.J., and De Felice, L.J. (2012). 4-(4-(dimethylamino)phenyl)-1-methylpyridinium (APP+) is a fluorescent substrate for the human serotonin transporter. The Journal of biological chemistry *287*, 8852-8863.

Sonders, M.S., Zhu, S.J., Zahniser, N.R., Kavanaugh, M.P., and Amara, S.G. (1997). Multiple ionic conductances of the human dopamine transporter: the actions of dopamine and psychostimulants. J Neurosci *17*, 960-974.

Sulzer, D., Sonders, M.S., Poulsen, N.W., and Galli, A. (2005). Mechanisms of neurotransmitter release by amphetamines: a review. Prog Neurobiol *75*, 406-433.

Vaughan, R.A. (2004). Phosphorylation and regulation of psychostimulant-sensitive neurotransmitter transporters. The Journal of pharmacology and experimental therapeutics *310*, 1-7.

Yamashita, A., Singh, S.K., Kawate, T., Jin, Y., and Gouaux, E. (2005). Crystal structure of a bacterial homologue of Na+/Cl--dependent neurotransmitter transporters. Nature *437*, 215-223.

Zapata, A., Kivell, B., Han, Y., Javitch, J.A., Bolan, E.A., Kuraguntla, D., Jaligam, V., Oz, M., Jayanthi, L.D., Samuvel, D.J., *et al.* (2007). Regulation of dopamine transporter function and cell surface expression by D3 dopamine receptors. The Journal of biological chemistry *282*, 35842-35854.

Zhao, C., Stolzenberg, S., Gracia, L., Weinstein, H., Noskov, S., and Shi, L. (2012). Ion-controlled conformational dynamics in the outward-open transition from an occluded state of LeuT. Biophysical journal *103*, 878-888.

Zhao, Y., Terry, D., Shi, L., Weinstein, H., Blanchard, S.C., and Javitch, J.A. (2010). Single-molecule dynamics of gating in a neurotransmitter transporter homologue. Nature *465*, 188-193.

Zhao, Y., Terry, D.S., Shi, L., Quick, M., Weinstein, H., Blanchard, S.C., and Javitch, J.A. (2011). Substrate-modulated gating dynamics in a Na+-coupled neurotransmitter transporter homologue. Nature *474*, 109-113.

Zhen, J., Chen, N., and Reith, M.E. (2005). Differences in interactions with the dopamine transporter as revealed by diminishment of Na(+) gradient and membrane potential: dopamine versus other substrates. Neuropharmacology *49*, 769-779.

Molecular Pharmacology Fast Forward. Published on April 21, 2014 as DOI: 10.1124/mol.114.091926
This article has not been copyedited and formatted. The final version may differ from this version.

FOOTNOTES

This work was supported by National Institutes of Health Grants [DA011697], MEG, [DA028112 and DA026947], LJD, and [5T32DA007281], RF.

Margaret E. Gnegy

Department of Pharmacology

2220E MSRBIII

University of Michigan Medical School

Ann Arbor, MI 48109-0632

Telephone: 734-763-5358

Fax: 734-763-4450

Email: pgnegy@umich.edu

† Rheaclare Fraser and Yongyue Chen contributed equally to this work.

Molecular Pharmacology Fast Forward. Published on April 21, 2014 as DOI: 10.1124/mol.114.091926
This article has not been copyedited and formatted. The final version may differ from this version.

FIGURE LEGENDS

Fig. 1. Expression of WT-, T62A-, and T62D-hDAT mutants causes similar membrane depolarization in *Xenopus* oocytes. *X.* oocytes were injected with 23 ng of cRNA for WT, T62A or T62D hDAT. Expression of hDAT statistically reduces the recorded resting membrane potential (RMP) of oocytes when compared to control oocytes injected with 23nl or water (***, $p < 0.001$).

Fig. 2. Dopamine-induced inward currents in T62D-hDAT oocytes are partially rescued by zinc. A. Representative continuous traces of currents measured in oocytes clamped at -60 mV are shown. Inward currents are observed in WT- and T62A-hDAT oocytes after application of 10 µM dopamine (DA). Co-application of 2 µM $ZnCl_2$ partially restored a measurable inward current in T62D-hDAT oocytes. **B.** Shows the change in accumulated current (Δ current = DA current – baseline current) in WT-, T62A-, and T62D-hDAT oocytes held at -60 mV. The data are expressed as the average ± s.e.m with numbers of oocytes for each condition given. Unpaired *t*-test with Welch's correction for DA ± zinc application shows a significant increase in the DA-induced currents in WT- (* $p < 0.05$), T62A- (***, $p < 0.001$), and T62D-hDAT (***, $p < 0.001$) expressing oocytes. Zinc did not affect the DA current measurement in control oocytes.

Fig. 3. Current-voltage relationships in hDAT expressing *Xenopus* oocytes. A step voltage clamp protocol was used from -150 to 30 mV at a holding potential of -60 mV and 10 mV step increments for 30 sec duration. Oocytes were challenged with 10 µM DA ± 2µM $ZnCl_2$. The current is displayed as the difference from baseline measured in the absence of substrate (ΔI). At hyperpolarizing potentials, DA (black squares) induces an inward current in **A**. WT- and **B.** T62A-hDAT oocytes. Co-application with zinc (open squares) potentiates DA induced inward

Molecular Pharmacology Fast Forward. Published on April 21, 2014 as DOI: 10.1124/mol.114.091926
This article has not been copyedited and formatted. The final version may differ from this version.

currents. **C.** In T62D-hDAT oocytes, DA inward currents are only measurable in the presence of zinc. Application of zinc alone (open circles) produced a small current in all constructs. Each I-V plot was generated from 4-6 oocytes expressing the indicated hDAT construct.

Fig. 4. Affinity of the fluorescent substrate, ASP^+ is unaffected by the T62A or T62D hDAT mutations. As detailed under Materials and Methods, **A.** uptake of 10 nM [^{3}H]DA for 3 min or **B.** binding of [^{3}H]WIN35,428 for 30 min in WT- (■), T62A- (▲), and T62D-(◊) hDAT HEK cells was measured as a function of varying ASP^+ concentrations. Data are expressed as the percent of the control without ASP^+; and are shown as the mean ± s.e.m, n = 2 experiments performed in triplicate. The IC_{50} (μM) values with 95% confidence intervals are reported in the text of the Results.

Fig. 5. Accumulation of fluorescent substrate, ASP^+ in T62A- and T62D-hDAT HEK cells. Representative confocal images of time dependent ASP^+ accumulation are displayed in columns **A.** WT-, **B.** T62A-, and **C.** T62D-hDAT, and **D.** parental HEK cells. Acquired representative images, of DIC and ASP^+ signals are overlain, at times 0 and 180 sec after exposure to 2 μM ASP^+. **E.** The optical density of the fluorescent signal was quantified in intracellular regions of WT- (■), T62A- (▲), T62D- (◊) hDAT, and parental (□) HEK cells using ImageJ software. Data are plotted for the full 3 min image acquisition of 10 sec intervals, WT, n = 140 cells, T62A, n = 126 cells, T62D, n = 148 cells and HEK, n = 148 cells.

Fig. 6. The reliance for extracellular Na^+ to promote DA uptake is not altered by the Thr62 hDAT mutations. Extracellular sodium (Na^+_e) stimulation of [^{3}H]DA uptake in WT- and T62 mutant hDAT HEK cells. Uptake of 10 nM [^{3}H]DA was conducted for 3 min at room temperature. Na^+ in the uptake buffer was replaced with NMDG-Cl to maintain osmolarity. The

Molecular Pharmacology Fast Forward. Published on April 21, 2014 as DOI: 10.1124/mol.114.091926
This article has not been copyedited and formatted. The final version may differ from this version.

IC_{50} (mM) for Na^+_e in WT- (■), T62A- (▲), and T62D- (◊) hDAT was 39.6, 40.5, and 58.7, respectively. Data are from n = 4 experiments done in triplicate and reported as a percentage of the maximum uptake achieved at the normal, highest [Na^+_e] tested.

Fig.7. Initial [^{3}H]DA efflux in T62D-hDAT is Na^+ independent and resembles inducible DA efflux of WT-hDAT HEK cells. A. WT-, **B.** T62A- and **C.** T62D-hDAT HEK cells were preloaded with 0.5 µM [^{3}H] DA (in normal KRH buffer) for 20 min. Basal and AMPH-induced DA efflux were determined while varying [Na^+_e]. After 15 min cells were stimulated with AMPH (10 µM, black arrow) in varying [Na^+_e] for 5 min. Data are averaged from 3-6 experiments performed in 3 or 4 replicates. In WT (**A**) and T62A (**B**), ** $p < 0.01$ for 0 versus 125 mM for basal DA efflux at times 5, 10, and 15 min; +++ $p < 0.001$, ++ $p < 0.001$, or + $p < 0.05$ for AMPH-induced DA efflux at 20 min compared to 15 min (before AMPH) at each corresponding [Na^+_e] **D.** Comparisons of basal and AMPH (black arrow) DA efflux in WT- (circles) and T62D-(squares) at 0 mM (open symbols) and 125 mM (closed symbols) Na^+_e. To account for variation in DA uptake, the data are represented as a percentage of the total [^{3}H] DA inside of the cell after DA preloading. Analyses of the 3-way interaction *(time · [Na^+_e] · cell type)* is not significantly different between WT and T62D at 0 mM Na^+ (with the exception of 15 min, $p = 0.005$). DA efflux after AMPH (20 min) is significantly greater in WT compared to T62D at 125 mM Na^+ ($p < 0.0001$), with no difference between cell types at 0 mM Na^+ ($p = 0.23$). The effect of Na^+_e on DA efflux *(time · cell type · [Na^+_e])* was significant in WT- ($p \leq 0.001$) but not in T62D-hDAT. Analyses of *cell type · [Na^+_e] · time* shows a significant change after the addition of AMPH (15 min vs. 20 min) in WT-hDAT at both 0 mM ($p = 0.002$) and 125 mM Na^+ ($p < 0.0001$); and in T62D at 0 mM Na^+ ($p = 0.03$), but not 125 mM ($p = 0.235$).

Figure 1

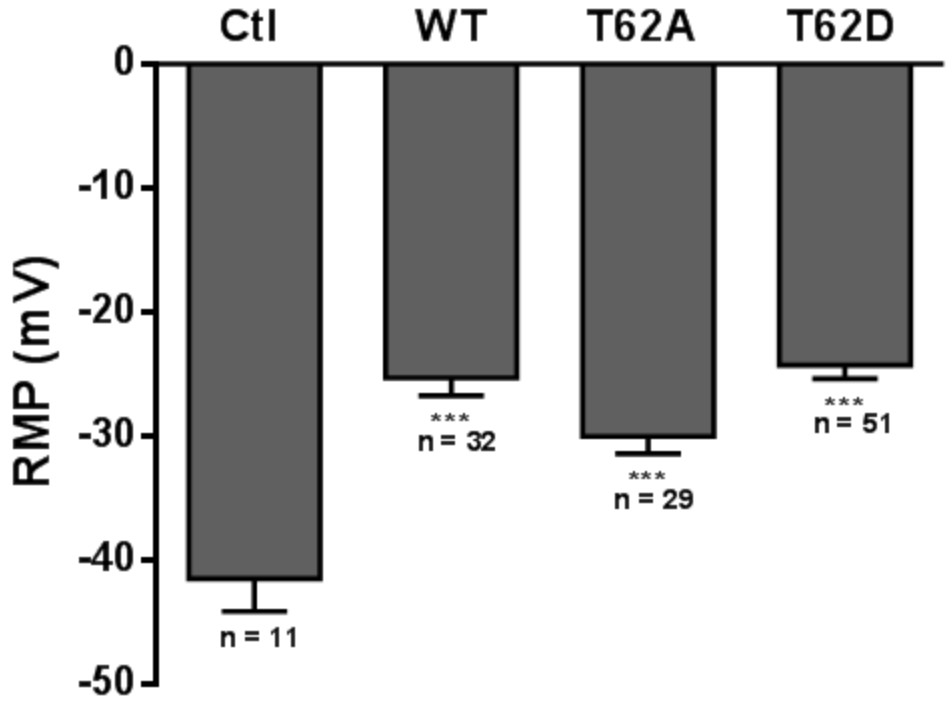

Figure 2

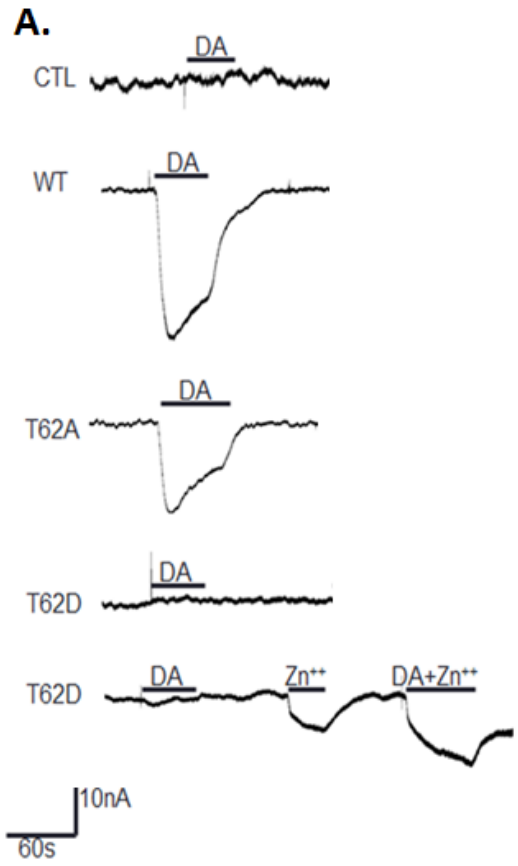

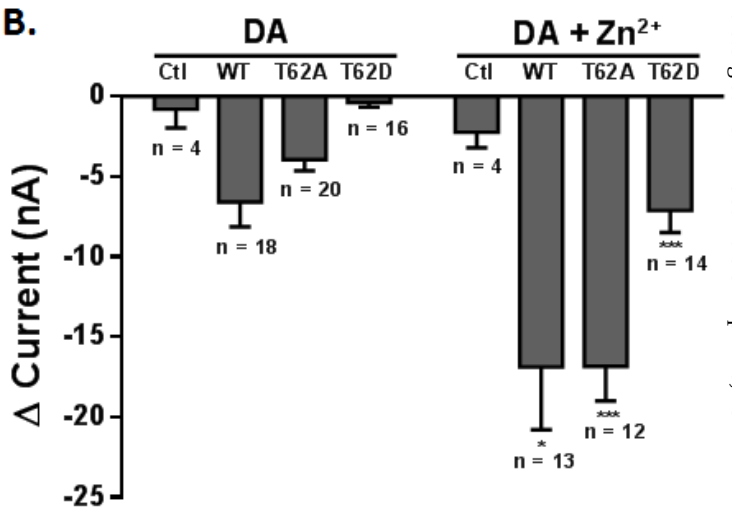

Figure 3

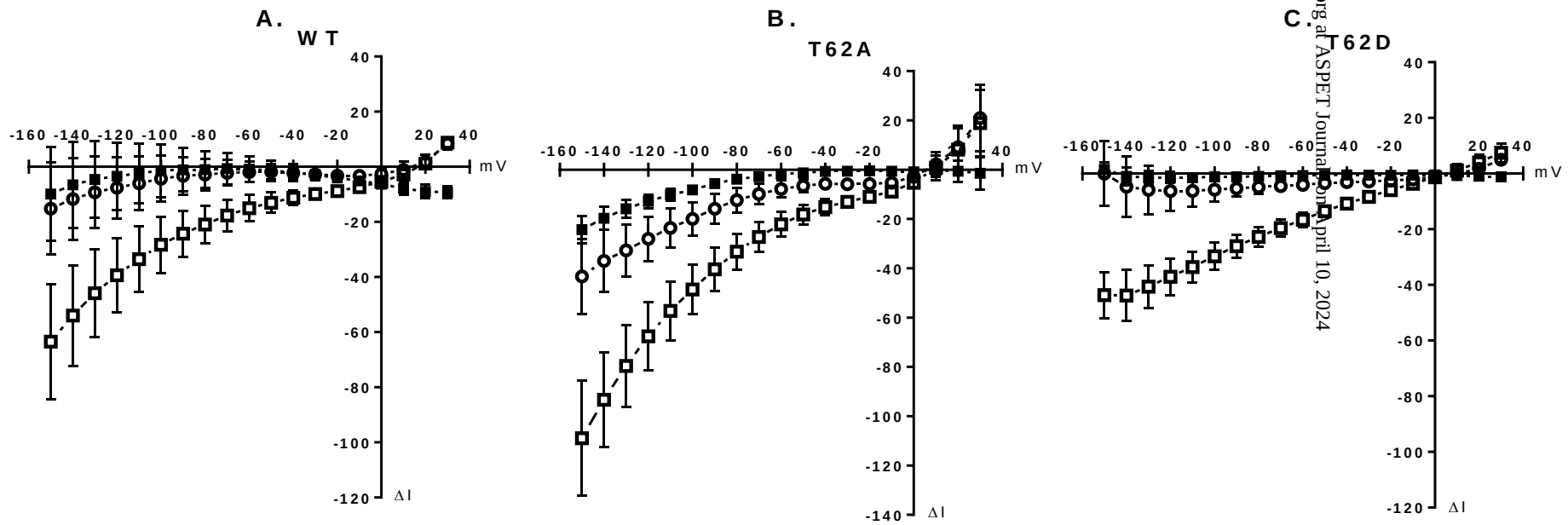

Figure 4

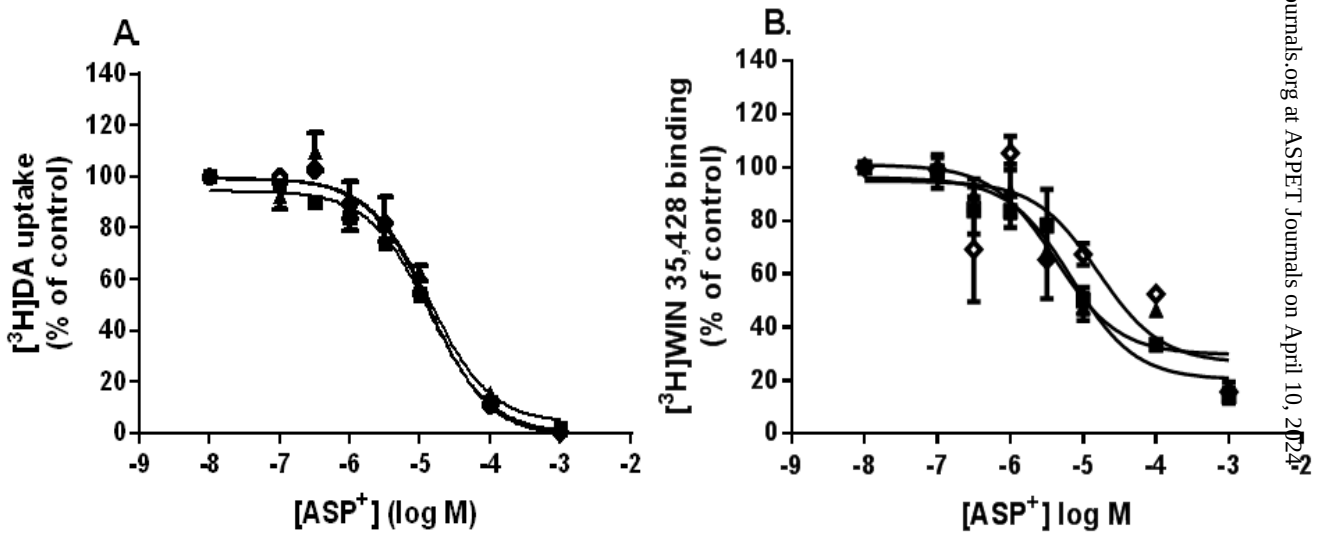

Figure 5

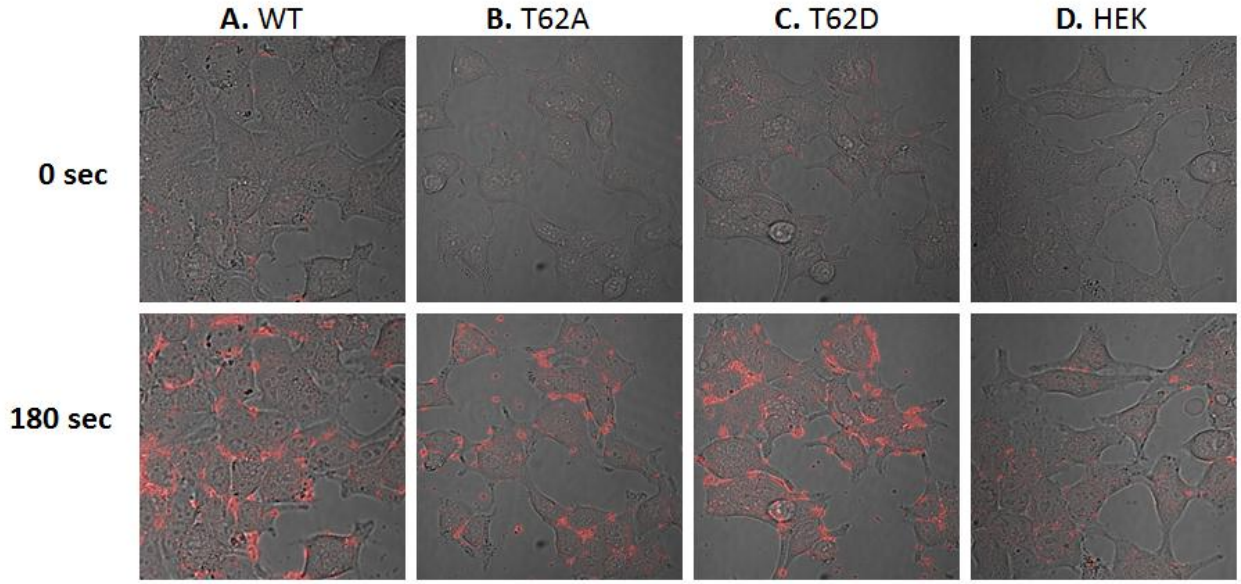

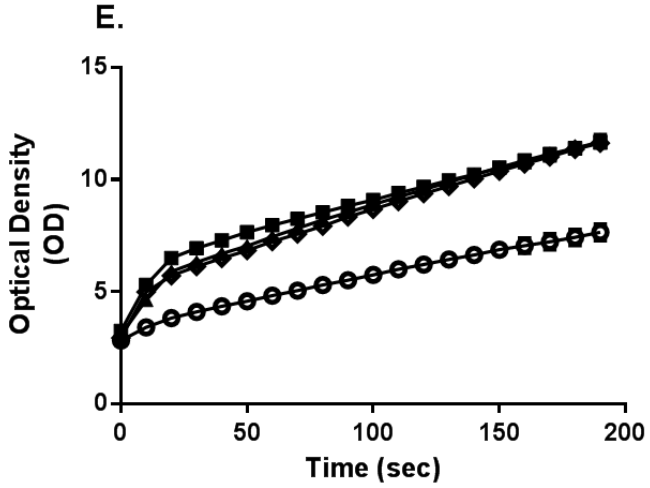

Figure 6

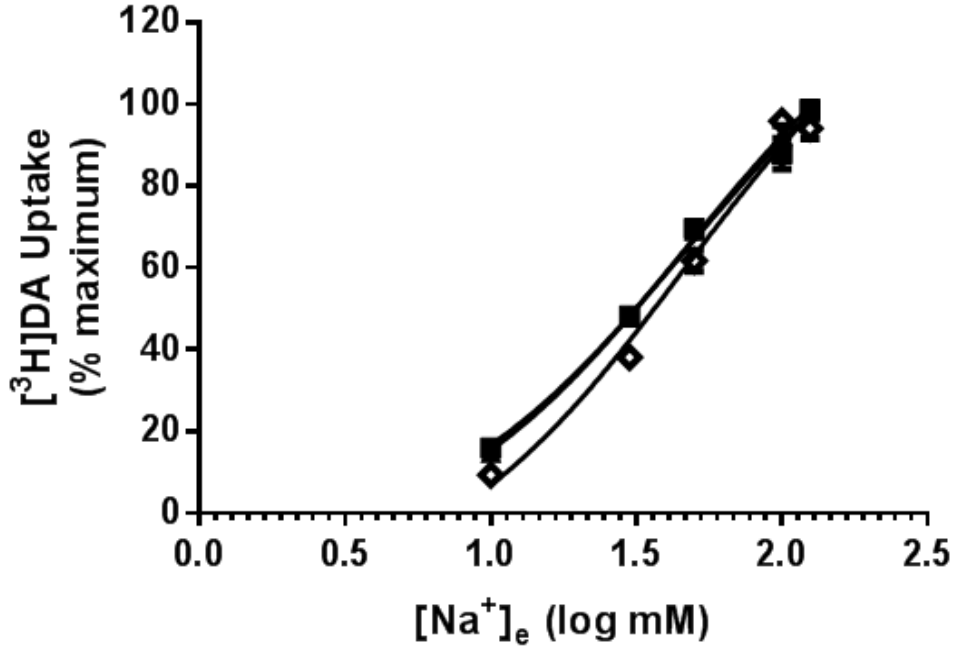

Figure 7